Insulin–Dendrimer Nanocomplex for Multi-Day Glucose-Responsive Therapy in Mice and Swine

Sijie Xian,[1,#] Yuanhui Xiang,[1,#] Dongping Liu,[1] Bowen Fan,[1] Katarína Mitrová,[2] Rachel C. Ollier,[1] Bo Su,[1] Muhammad Ali Alloosh,[3] Jiří Jiráček,[2] Michael Sturek,[3] Mouhamad Alloosh,[3] Matthew J. Webber[1,*]

1- University of Notre Dame, Department of Chemical & Biomolecular Engineering, Notre Dame, IN 46556 USA

2- Czech Academy of Sciences, Institute of Organic Chemistry and Biochemistry, Prague, 16610 Czech Republic

3- Corvus Biomedical, LLC, Crawfordsville, IN 47933 USA

[#]- S.X. and Y.X. contributed equally to this work

*- Correspondences addressed to: mwebber@nd.edu

Abstract: The management of diabetes in a manner offering autonomous insulin therapy responsive to glucose-directed need, and moreover with a dosing schedule amenable to facile administration, remains an ongoing goal to improve the standard of care. While basal insulins with reduced dosing frequency, even once-weekly administration, are on the horizon, there is still no approved therapy that offers glucose-responsive insulin function. Herein, a nanoscale complex combining both electrostatic and dynamic-covalent interactions between a synthetic dendrimer carrier and an insulin analogue modified with a high-affinity glucose-binding motif yields an injectable insulin depot affording both glucose-directed and long-lasting insulin availability. Following a single injection, it is even possible to control blood glucose for at least one week in diabetic swine subjected to oral glucose challenges. Measurements of serum insulin concentration in response to challenge show increases in insulin corresponding to elevated blood glucose levels, an uncommon finding even in preclinical work on glucose-responsive insulin. Accordingly, the subcutaneous nanocomplex that results from combining electrostatic and dynamic-covalent interactions between a modified insulin and a synthetic dendrimer carrier affords a glucose-responsive insulin depot for week-long control following a single routine injection.

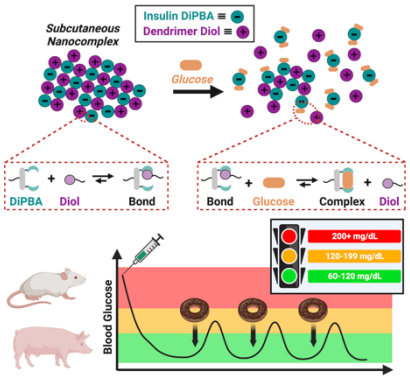

Keywords: Drug Delivery; Nanotechnology; Materials Chemistry; Bioconjugation

Introduction

Diabetes is among the most pressing global healthcare challenges. The incidence of all forms of diabetes is increasing,[1,2] coupled with extensive suffering, comorbidity, and economic burden.[3] The absence or dysfunctional signaling of insulin, a hormone secreted by the pancreas in response to elevated blood glucose levels that triggers glucose uptake and storage,[4] is central to the pathology of diabetes. Exogenous insulin is critical to manage type 1 diabetes, and is often also used in later stages of type 2 diabetes.[5] Insulin is typically self-administered, with best outcomes following a strict treatment regimen. Some individuals respond well to insulin therapy, yet many still suffer complications that arise from poor adherence or from inadequate glycemic control.[6] An overdose of insulin can lead to acute hypoglycemia, with serious and even lethal outcomes.[7] For this reason, insulin is often under-dosed so as to avoid the acute risks from overdose. Unfortunately, prolonged blood glucose instability and hyperglycemia that arises from under-dosing insulin leads to its own chronic comorbidities, including cardiovascular and neurological diseases, retinopathy, nephropathy, and non-healing wounds.[3] Diabetics also have an increased rate of total, cardiovascular, and cancer mortality.[8] There is thus a growing need to improve blood glucose control and avoid the acute and chronic health complications that arise from blood glucose instability.

Progress in diabetes treatment has been realized by insulin variants with tunable pharmacokinetics,[9,10] as

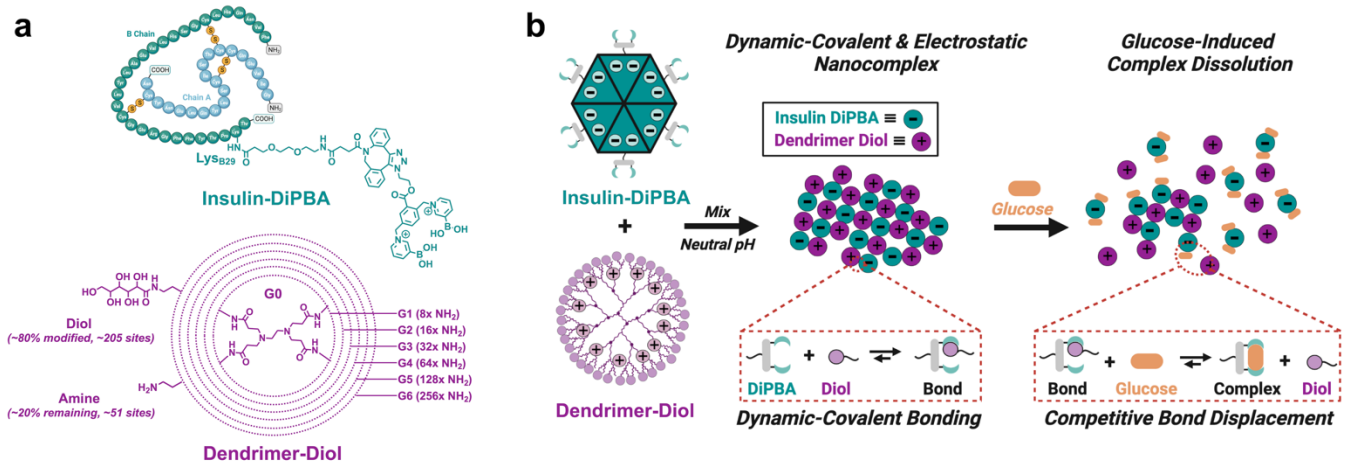

Figure 1: (a) Chemical structures of Insulin-DiPBA, site-specifically modified at the B29 lysine with a glucose-binding diboronate motif, and generation 6 (G6) PAMAM Dendrimer-Diol, modified on its periphery with glucose-like diol molecules. **(b)** When the net-negative Insulin-DiPBA and positive Dendrimer-Diol are mixed, a combination of electrostatic interactions and DiPBA–diol dynamic-covalent bonding yields formation of a nanocomplex; this DiPBA–diol bonding of the complex is susceptible to competition from glucose driving its dissolution and insulin release from the nanocomplex.

well as advances in pumps, continuous glucose monitors, and related hardware.[11,12] Key developments in recent decades include the approval of insulin variants with either rapid-acting (prandial) and long-lasting (basal) function. Current clinically used basal variants offer ~1 day of blood glucose support (e.g., *Insulin Glargine* and *Insulin Detemir*), though nascent week-long variants fused to antibody Fc domains (*Insulin Efsitora Alfa*) or that bind with very high affinity to circulating albumin (*Insulin Icodec*) are on the cusp of clinical use.[10] While day- and week-long variants offer basal support with enhanced duration and ease of use, these do not adjust bioavailability or potency as a function of blood glucose level.

Glucose-responsive therapy remains a key goal in the development of materials and formulations for insulin delivery.[13–15] This approach would vary dosage according to real-time disease state (*i.e.,* glucose level), delivering on a vision of a synthetic "closed-loop" therapy that senses changes in blood glucose and responds by tuning the bioavailability and/or potency of insulin.[16] Glucose sensing is typically achieved by integrating one of three mechanisms into materials design: (i) enzyme-catalyzed pH change, (ii) glucose-binding proteins, or (iii) glucose-binding synthetic motifs.[17] However, recreating the natural dynamics of glycemic control, with both peaks and troughs, is still a major challenge in the materials-based approaches explored thus far. Moreover, managing diabetes necessitates life-long therapy; glucose-responsive technologies must be amenable to serial self-administration with practical dosing schedules. As such, and in spite of decades of progress, there is so far limited demonstration of systems that tune insulin bioavailability/potency according to real-time need so as to meet both basal and prandial insulin requirements in a single platform.

Herein, an insulin–dendrimer formulation is reported that combines electrostatic complexation with added dynamic-covalent interactions susceptible to competition from free glucose to form a durable subcutaneous nanocomplex depot (***Fig 1***). Phenylboronic acids (PBAs) are synthetic motifs long-explored for glucose-responsive materials.[18–20] Yet, PBAs do not bind glucose with high affinity or specificity; K_{eq} for glucose-binding of a common PBA motif of 8.6 M^{-1} is well below what would be expected to reliably function at physiological glucose concentrations of ~5-10 mM.[21,22] A pyridinium diboronate (DiPBA) motif was recently reported to bind glucose with an affinity of 1295 M^{-1} through bidentate interactions while also affording improved glucose specificity.[22] In this present work, DiPBA was site-specifically conjugated to the B29 lysine residue of insulin by copper-free click chemistry (***Fig 1a***). Polyamidoamine (PAMAM) dendrimers, with a long history of use in drug delivery,[23–25] were used at generation six (G6) and peripherally modified with a corresponding diol on the majority of the terminal amines. The enhanced affinity and specificity of the DiPBA was intended to enable glucose-responsive and glucose-specific bonding to diols on the dendrimer, to further stabilize the electrostatic complex between the net-negative insulin and the positively charged dendrimer. When these two components were mixed at a charge-balanced ratio, a nanocomplex resulted when at neutral pH (***Fig 1b***); the extent of complex formation

was reduced without the inclusion of DiPBA–diol dynamic-covalent bonding. The nanocomplexes exhibit glucose-directed solubility and responsive insulin release. These features translate to a long-lasting subcutaneous depot that forms upon injection and enables blood glucose correction for ~5 days in diabetic mice and at least one week in diabetic swine, with both species having increased bioavailability of insulin in response to elevated glucose levels.

Results & Discussion

Material Design & Synthesis. The design inspiration for this approach took concepts from three different clinically evaluated insulin therapeutics to achieve a long-lasting and glucose-responsive depot. A leading option for basal insulin therapy, *Insulin Glargine*, forms a depot by subcutaneous nanoprecipitation following injection in a pH 5 suspension as a result of its roughly neutral isoelectric point; slow enzymatically driven depot re-solubilization offers protracted basal availability and ~24-36 h duration of action.[26–28] *NPH Insulin*, an intermediate-acting insulin with clinical use dating back to the 1940s, forms a depot with ~24 h duration of action with protraction from the electrostatic complexation of insulin and a positively charged biopolymer protamine.[26–28] Meanwhile, the first glucose-responsive insulin used pre-clinically (*MK-2640*) modified insulin with oligosaccharides to leverage sugar-binding proteins as depots for competition-mediated displacement and insulin release.[29] As such, the envisioned design here (***Fig 1***) was intended to couple features of subcutaneous nanoprecipitation, electrostatic complexation with a macromolecular carrier, and molecular scale interactions susceptible to competition from free glucose to yield a long-lasting *AND* glucose-responsive insulin depot.

Insulin was first modified with the reported DiPBA motif to endow prosthetic glucose-responsive functionality (***Fig S1-S6***). Detailed synthetic methods can be found in ***Section S.1*** of the online supporting information. Insulin has three primary amines for modification; reaction at the ε-amine of the B29 lysine residue can be enhanced relative to the primarily amines of the A1 and B1 N-terminal positions by controlling the pH of the amide bond-forming reaction.[30] The B29 lysine is also where insulin is modified with a C_{14} myristic acid in *Insulin Detemir*, a clinically used long-lasting basal variant.[31] The direct modification of the ε-amine of the B29 lysine using a related DiPBA motif bearing a carboxylic acid was not feasible at pH 11 due to DiPBA degradation, likely by protodeboronation,[32] under basic reaction conditions. As such, a two-step approach was implemented wherein insulin was first modified with Dibenzocyclooctyne-PEG_2-N-hydroxysuccinimidyl ester (DBCO-PEG_2-NHS ester) under pH 11 conditions, and then subsequently a DiPBA-azide compound (***Fig S4***) could be attached *via* strain-promoted alkyne–azide cycloaddition, or so-called copper-free "click" chemistry (***Fig 1a***). Reversed phase preparative HPLC was performed after both DBCO and DiPBA modification steps to isolate the single-modified insulin product. The effectiveness of site-specific modification by this two-step approach was confirmed using digestion of insulin with DTT and trypsin followed by high-resolution LC-MS/MS analysis of the three resulting peptide fragments, which confirmed exclusive DBCO modification at the B29 site (***Fig S5***). The ensuing "click" reaction proceeds readily to produce the final DiPBA-modified product (***Fig S6***). Overall, this procedure results in a 33% yield of Insulin-DiPBA from recombinant human insulin.

The activity of Insulin-DiPBA was next assessed through an *in vitro* cell activity assay (***Fig S12***). This assay, performed in model C2C12 myoblast cells,[33] quantifies insulin receptor activation reflected in phosphorylated AKT (pSer473) vs. total AKT. The EC_{50} measured by this assay was 13 µg/L for recombinant insulin; addition of a DBCO linker led to an increase in EC_{50} of an order of magnitude (101 µg/L), with subsequent DiPBA addition having similar impact on in vitro potency (EC_{50} 89 µg/L). Thus, modification with DBCO led to reduced insulin potency *in vitro* that was maintained upon subsequent DiPBA attachment *via* click chemistry. As cell assays were performed in glucose-containing media, the DiPBA would appear to still signal in its glucose-bound state, though the modification itself does impact activity. In another measure of insulin activity/potency, Insulin-DiPBA alone was assessed in STZ diabetic mice (***Fig S13***). At an identical dose of 0.1 mg/kg (equal to 3 IU/kg of native insulin), Insulin-DiPBA depressed blood glucose at a rate comparable to unmodified insulin in the first 90 min after administration, suggesting potency to be initially matched. Yet, whereas blood glucose increased in the insulin group after ~120 min, Insulin-DiPBA had a longer duration of action with blood glucose rising much more slowly after an initial nadir at ~150 min. Such protraction is common when receptor binding affinity is reduced, owing to the reduced rate of insulin clearance from circulation;[10] the physicochemical modification of insulin may also interfere with the binding of insulin-degrading enzyme to its substrate.[34] As such, modification may be responsible for extending the duration of action relative to unmodified insulin *in vivo*, though does not appear to have a

dramatic impact on potency reflected in the initial rate of blood glucose correction

To further understand the impact of DiPBA modification on insulin receptor affinity, radiolabelled displacement studies were performed to assess the affinity of these B29-modified insulins in binding to insulin receptor A (IR-A) and insulin receptor B (IR-B). The affinities of Insulin-DBCO and Insulin-DiPBA in binding to IR-A were 38% and 32% that of native insulin, respectively; for IR-B, these were also reduced to 50% and 42% of native insulin (***Fig S14***). *Insulin Detemir* also has reduced potency due to insulin receptor binding affinity that is ~25% that of unmodified insulin,[35] pointing to the expected impact of B29 modification on insulin potency.[36] As such, the reduced affinity arising from B29 modification aligns with expectations, and is likely to underlie the reduced cell signaling potency and *in vivo* protraction of function observed. Modifying insulin can also unintentionally increase mitogenicity of the protein *via* aberrant activation of insulin-like growth factor receptor (IGF-1R). For example, the modification of the C-terminal B chain in *Insulin Glargine* is known to enhance mitogenicity through IGF-1R binding.[37,38] However, here the B29 modification actually resulted in lower binding affinity for IGF-1R than even unmodified human insulin (***Fig S14***); mitogenicity *via* IGF-1R binding is therefore unlikely. Yet, as mitogenicity of insulin is mechanistically complex,[39] it is possible that synthetic modification of insulin may still enhance its mitogenicity through some other mechanism and this topic would need to be further explored in development of any therapeutic insulin.

As insulin has a net-negative charge, PAMAM dendrimers were chosen as carriers to leverage their cationic character in facilitating electrostatic complexation. The predictable and globular structure of PAMAM dendrimers, with very low polydispersity, was specifically targeted for this work due to protein-mimetic size and structural features to ensure reproducible function of this envisioned nanocomplex platform. These dendrimers also have well-defined and addressable end-groups for facile modification.[23] PAMAM dendrimers of Generation 2, 4, and 6 were next modified by reaction with glucano-**δ**-lactone (GdL) on their peripheral amino groups, following methods used for the preparation of hydrogels using PBA–diol bonding.[40] In each case, ~80% of terminal amines were modified with the GdL-derived diol, as confirmed by ^{1}H NMR (***Fig S7-S9***). Both Insulin-DiPBA and the G6 Dendrimer-diol exhibited excellent cytocompatibility *in vitro* (***Fig S15***).

Nanocomplex Formation. Two complementary interactions were envisioned to prepare Insulin–Dendrimer nanocomplexes. The inherent differences in net charge were first targeted to drive nanoprecipitation and depot formation when the net-negative Insulin-DiPBA and positive Dendrimer-Diol were mixed, similar to the mechanism underlying function of *NPH Insulin*. Added to that was the dynamic-covalent DiPBA–diol interaction to stabilize the Insulin–Dendrimer nanocomplexes and render their interactions glucose-responsive. To first confirm that Insulin-DiPBA retained its ability to recognize the GdL-derived diol, isothermal titration calorimetry (ITC) was performed at pH 7.4 to assess binding between Insulin–DiPBA and a small molecule GdL-derived diol (***Fig S16***). The binding affinity (K_{eq}) was measured to be 2.3 x 10^4 M^{-1} at pH 7.4. Interestingly, this is ~4 times higher affinity than was measured for the small molecule DiPBA–diol interaction.[22] Attachment to insulin could alter both the presentation and associative dynamics for the dynamic-covalent interaction, giving rise to higher binding affinities.

Insulin-DiPBA and Dendrimer-Diol mixtures were soluble at pH 5, yet formed visible precipitates at pH 7.4, noted by increased sample turbidity (***Fig 2a***). This solubility profile is similar to that of *Insulin Glargine*, which is injected at pH 5 and forms a nanoprecipitate depot in the body due to its neutral isoelectric point.[26–28] The pH-induced shift in solubility likely results from enhanced electrostatic screening at neutral conditions as well as higher affinity DiPBA–diol bonding. The latter point is supported by the pH dependence of the bonding between Insulin-DiPBA and GdL-derived diol, where affinity measured by ITC was reduced by an order of magnitude (2.8 x 10^3 M^{-1}) at pH 5, and no binding was recorded at pH 3 (***Fig S16***). The pKa for the two boronic acids on the DiPBA was previously reported to be 4.5 ($pK_{a,1}$) and 7.4 ($pK_{a,2}$).[22] PBA–diol interactions are well-known to form readily at pH levels at or above the pK_a of the boronate, wherein it can adopt its tetrahedral and charged conformation.[17] As such, these pH-dependent trends in affinity are expected.

Alone at pH 7.4, Insulin-DiPBA and Dendrimer-Diol were fully soluble with no measurable turbidity (***Fig S17***). The mixing of Dendrimer-Diol (+) and Insulin–DiPBA (-) under these same conditions revealed maximal complex formation at a charge ratio of 1:1, as evidenced by a measurement of sample turbidity over a range of mixing ratios (***Fig 2b***). Both Insulin-DiPBA and Dendrimer-Diol were essentially fully incorporated in the formed nanocomplexes at 1:1 charge balance, as verified by analysis of the soluble fraction following separation of the formed complexes *via* centrifugation (***Fig S18***). For clarity, the molar ratio of Dendrimer-Diol to Insulin-DiPBA is 1:17 at

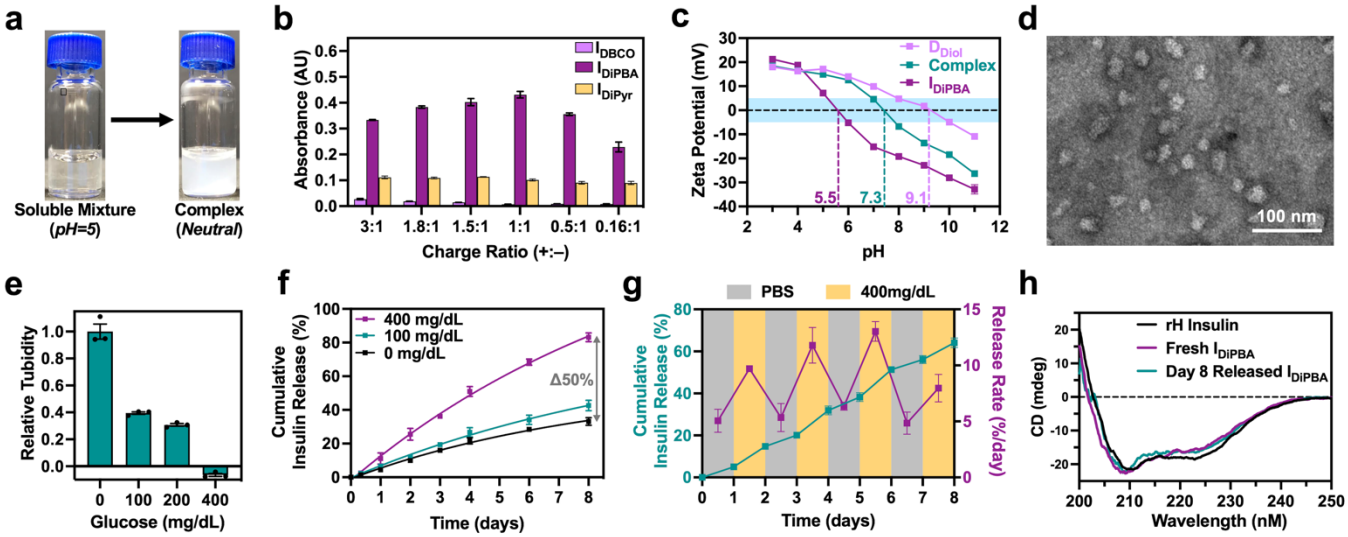

Figure 2: (a) The mixture of Insulin-DiPBA and Dendrimer-Diol is soluble and translucent at pH 5, but precipitates under neutral conditions. **(b)** Tuning the ratio of positive charge, originating from the Dendrimer-Diol, to negative charge from the Insulin-DiPBA enables precipitation to be optimized, as measured by sample turbidity (n=3/ratio/group, mean ± SD shown). **(c)** The zeta potential of each component, as well as that for the 1:1 charge ratio mixture (*complex*) was measured over a range of pH to estimate isoelectric points (*dashed vertical lines)* where zeta potential is 0 (n=3/titrations/group, mean ± SD shown). **(d)** Negative-stained transmission electron microscopy visualizing the nanocomplexes resulting from the 1:1 charge ratio mixture of Insulin-DiPBA and Dendrimer-Diol. **(e)** Relative turbidity of the 1:1 charge ratio mixture of Insulin-DiPBA and Dendrimer-Diol prepared at different glucose concentrations (n=3/group, mean ± SD shown). **(f)** Release of free Insulin-DiPBA from pre-formed complex in buffer conditions of 0 mg/dL, 100 mg/dL, and 400 mg/dL glucose (n=3/group, mean ± SD shown). **(g)** Cycling the nanocomplexes between conditions of no glucose (PBS, *gray*) and high glucose buffer (400 mg/dL, *yellow*), measuring cumulative insulin release as well as the release rate between each sampling point (n=3/group, mean ± SD shown). **(h)** Circular dichroism of released Insulin-DiPBA compared to fresh samples of Insulin-DiPBA and recombinant human insulin.

1:1 charge balance; this equates to a ratio of 1:2.8 in terms of moles of dendrimer to insulin hexamers. The method of calculating the average charge and charge ratio for these formulations is further elaborated upon in ***Section S.3*** of the *online supporting information*. Control insulin variants consisting of Insulin-DBCO and insulin modified with a dipyridinium prosthetic group (Insulin-DiPyr) did not form the same level of complex formation at any charge ratio, supporting a role for DiPBA–diol crosslinking alongside electrostatics in stabilizing the nanocomplex. When peripheral amines on the Dendrimer-Diol were converted to carboxylic acids, effectively canceling the charge on the dendrimer, complexation still occurred when mixing with Insulin-DiPBA at the same molar ratio as the 1:1 complex though not to the same extent on the basis of turbidity (***Fig S19***). The data for nanocomplexation, together with ITC studies, point to DiPBA–Diol interactions being the primary means of nanocomplexation, with electrostatics serving in a stabilizing role. G6 PAMAM dendrimers (~58 kDa) have a diameter of ~6.7 nm,[41] roughly comparable to the dimensions of an insulin hexamer (~36 kDa) with a diameter of ~5.6 nm.[42] The assumption of a hexameric state for Insulin-DiPBA was supported by dynamic light scattering (***Fig S20***), comparing diffusion coefficients to that for native insulin without zinc removed as well as results in published work.[43] As such, from the outset G6 PAMAM dendrimers were hypothesized to be a better match to formulate with insulin for depot formation. This was further confirmed when comparing the resulting nanoprecipitation to that from other amine-terminated PAMAM generations (G2 and G4), which had reduced turbidity even at a state of charge balance (***Fig S21***).

Zeta potential collected in the course of a pH titration revealed isoelectric points of ~5.5 for Insulin-DiPBA and ~9.1 for the Dendrimer-Diol, with the 1:1 charge-balanced complex being net-neutral at pH ~7.3 (***Fig 2c***). These data further support the methods used to estimate the charge state of the two components to achieve balance, confirming electrostatic stabilization under neutral pH conditions. Nanocomplex diameters of ~30-40 nm were observed by transmission electron microscopy in the dry state (***Fig 2d***); these diameters are on the same order as those formed by *Insulin Glargine* when introduced into neutral conditions.[44] When forming nanocomplexes in the presence of glucose, the extent of aggregation was reduced, with no detectable complex formed when glucose levels were raised to up to level of 400 mg/dL, resembling hyperglycemic conditions (***Fig 2e***). The impact on nanocomplex formation due to competition from glucose further supports a primary role for DiPBA–Diol dynamic-covalent interactions in the initial nanocomplex formation of the Insulin–Dendrimer

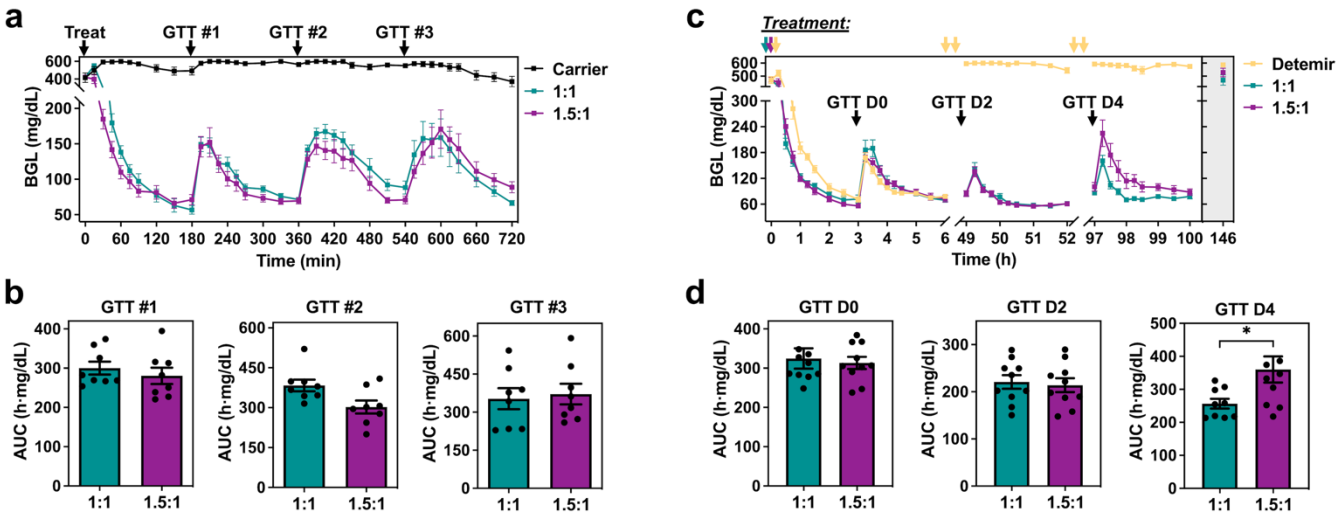

Figure 3: (a) Treatment of overnight-fasted STZ diabetic mice with carrier control (Dendrimer-Diol) or the Insulin-Dendrimer nanocomplex formulations at a charge ratio of 1:1 or 1.5:1. Following administration of treatment (t=0) three consecutive intraperitoneal glucose tolerance tests (IPGTT) were performed while maintaining mice in a fasted state (n=6 for carrier and n=8 for treatment groups, mean ± SEM shown). **(b)** The area under the curve (AUC) for each challenge was quantified to compare the response of the 1:1 and 1.5:1 formulations (n=8/group, mean ± SEM shown, no statistical significance). **(c)** In a separate study to assess long-term function, overnight-fasted STZ diabetic mice were administered Insulin-Dendrimer nanocomplex formulations at a charge ratio of 1:1 or 1.5:1 and compared to a potency-matched dose of clinically used *Insulin Detemir*. IPGTT was then performed at day 0 (D0). *Insulin Detemir* was serially dosed daily and mice were subjected to follow-up IPGTT were preformed again after a brief 3-hour fast on D2 and D4. On D6 following treatment with Insulin-Dendrimer nanocomplex formulations, hyperglycemia was restored in all mice (n=10/group, mean ± SEM shown). **(d)** AUC was quantified to compare the response of the 1:1 and 1.5:1 formulations (n=10/group, mean ± SEM shown, *-P<0.05 determined from Student's t-test).

formulation. When complexes were pre-formed and exposed to bulk conditions of 400 mg/dL, the release of free insulin was accelerated relative to its release in a bulk buffer without glucose or in buffer containing a normal (100 mg/dL) level of glucose (***Fig 2f***). Sustained release was observed in both cases, with total cumulative release after 8 days of ~83% in the 400 mg/dL case versus ~33% in buffer and ~43% in 100 mg/dL glucose. It is expected that some insulin release occurs even in the absence of glucose under these dilution conditions, resulting from a shift in the binding equilibrium of DiPBA–diol interactions as well as slow nanocomplex erosion. Importantly, the addition of protein to the release media (10% fetal bovine serum) to more closely match conditions *in vivo* had no impact on release (***Fig S22***). The release rate was also roughly doubled upon repeated cycling between no and high glucose levels (***Fig 2g***). Of note, when the complexes were compared at close to charge balance (+:- of 1.5:1), insulin release in both glucose-free and glucose-containing media was enhanced, with similar doubling of the release rates when cycled between no glucose and 400 mg/dL (***Fig S23***). Circular dichroism (CD) spectroscopy of Insulin-DiPBA after 8 days of release from the Insulin–Dendrimer nanocomplex revealed no change in characteristic α-helical secondary structure compared to freshly dissolved recombinant insulin or fresh Insulin-DiPBA (***Fig 2h***).

Blood Glucose Correction in Mice. Stable Insulin–Dendrimer nanocomplexes at charge ratios (+:-) of 1:1 and 1.5:1 were next explored for single day blood glucose correction in STZ-induced diabetic mice subjected to multiple glucose challenges. These two formulations were evaluated in tandem for early studies as they demonstrated the highest complexation by turbidity measurements along with glucose-responsive insulin release. The STZ mouse model recreates clinical features of hyperglycemia and insulin deficiency of type 1 diabetes.[45] The Insulin–Dendrimer formulations for these and subsequent rodent studies were performed at an optimal insulin dose of 10.4 mg/kg; details for how this dose was determined are found in ***Section S.4*** of the online supporting information. Complexes or a carrier control consisting of only the Dendrimer-Diol were injected subcutaneously (t=0) in overnight-fasted diabetic mice; both complexes restored blood glucose to within a normal physiological range (60-180 mg/dL for mice) over the ensuing 3 h after dosing (***Fig 3a***). Upon initial dosing, average blood glucose levels reached 57 mg/dL in the 1:1 treatment group; though mice remained stable and alert, these values indicate moderate hypoglycemia that may arise from some extent of insulin burst release upon injection and compression of the liquid formulation under the skin. By comparison, the same extent of hypoglycemia was not observed for the 1.5:1 formulation in this study, where the dendrimer carrier component was at a greater relative

ratio. The Dendrimer-Diol carrier control showed no impact on blood glucose, with these mice remaining hyperglycemic for the duration of the study. A control of Insulin-DiPBA at the same dose used in the Insulin–Dendrimer nanocomplex was not feasible, as alone this dose of Insulin-DiPBA is well in excess of its lethal dose; this likewise offers indirect support for retention of Insulin-DiPBA in the subcutaneous depot when combined with Dendrimer-Diol. Intraperitoneal glucose tolerance tests (IPGTT) were next performed every 3 h for three cycles while monitoring blood glucose. Both complexes corrected blood glucose following each of three administered IPGTT rounds, with normoglycemia still maintained at 12 h following treatment and three IPGTT cycles. Blood glucose levels at this point for the 1:1 (67 mg/dL) and 1.5:1 (89 mg/dL) formulations were well within the normal range for a fasted healthy mouse. Area under the curve (AUC) after each challenge was quantified (***Fig 3b***), showing comparable response for both formulations. AUC values were also comparable across all three IPGTT cycles.

Subcutaneous injection was chosen for evaluation of this technology, as the most effective and most used site for insulin due to consistent uptake in a self-administered setting.[46] However, for a glucose-responsive delivery approach, it is noted that interstitial glucose levels are typically lower than plasma glucose levels and have ~10 minutes of lag time in humans,[47] and alternate sites (*e.g.,* intramuscular) may thus be appropriate to consider. It is furthermore possible that interstitial glucose is able to disrupt the initial nanocomplex formation following injection. A comparison of data presented here for the full formulation at an Insulin-DiPBA dose of 10.4 mg/kg (***Fig 3a***) with data for Insulin-DiPBA alone at a dose of 0.1 mg/kg (***Fig S13***) reveals similar post-injection nadir values yet a much longer duration of action for the formulation, suggesting that any initial burst of insulin following injection is likely only a small fraction of the injected dose. Moreover, though the DiPBA structure was designed to be more glucose-specific than typical PBA chemistries,[22] and binds better to the diol presented on the dendrimer than it does to glucose (***Fig S16***), it likely also binds to diols or analytes in the tissue and this could also contribute to the displacement and release of Insulin-DiPBA *in vivo*.

Examples of insulin delivery approaches that correct blood glucose in response to multiple challenges in a single day have been previously reported.[22,30,48,49] Here, with sustained function at 12 h following treatment, a subsequent study was thus performed to test long-term glucose-responsive function of the Insulin-Dendrimer nanocomplex formulations subjected to glucose challenge on day 0, 2, and 4 (***Fig 3c***); these studies were performed against a control of daily administration of *Insulin Detemir*, a clinically used long-lasting basal insulin that achieves protraction by binding to circulating serum albumin.[31] The daily dosing of the *Insulin Detemir* control was chosen to be potency-matched to reach the same blood glucose level at 3 h after administration in overnight-fasted mice, similar to methods used to determine insulin potency in rabbits that form the basis of modern day "International Units" (IU) convention.[50] *Insulin Detemir* offered similar correction following the day 0 challenge in overnight-fasted mice, reaching blood glucose levels of 71 mg/dL after 3 h, which was comparable to treatment with the 1:1 (72 mg/dL) and 1.5:1 (60 mg/dL) complexes. However, the daily administration of *Insulin Detemir* did not sustain blood glucose control when this was not combined with overnight fasting. AUC values were quantified for the two formulations (***Fig 3d***), with the 1:1 charge complex demonstrating significantly greater responsiveness to IPGTT at day 4 following treatment. AUC values were also comparable across all days, and similar to the values obtained for the prior study with multiple IPGTT cycles administered in a single day. Though both ratios performed comparably, the significant improvement in response seen in AUC values for the 1:1 formulation at day 4 may be due to a lower excess of diol sites from less Dendrimer-Diol in the formulation, enhancing the ability of glucose to compete at later stages of the study when there is less Insulin-DiPBA remaining for competition-mediated release. By day 6, however, blood glucose had returned to a hyperglycemic state for mice that were treated with both the 1:1 and 1.5:1 Insulin–Dendrimer nanocomplexes (***Fig 3c***). However, treatment with both complexes demonstrated sustained blood glucose control for ~5 d with repeated response to IPGTT.

Glucose-Triggered Depot Insulin Release. Multi-day blood glucose control from Insulin–Dendrimer formulations with sustained reduction and responsive correction when subjected to IPGTT at least supports significant protraction of insulin from the depot, beyond that observed by most long-lasting basal insulins; it also exceeds that reported from DiPBA-based hydrogel delivery approaches, which only afforded blood glucose control for a single day.[22] Verifying authentic glucose-responsive depot function—and not just ultra-long-lasting insulin controlled release functionality—required further study of serum insulin concentrations in response to blood glucose challenge. Accordingly, serum insulin levels were monitored at 0, 2, and 4 d following

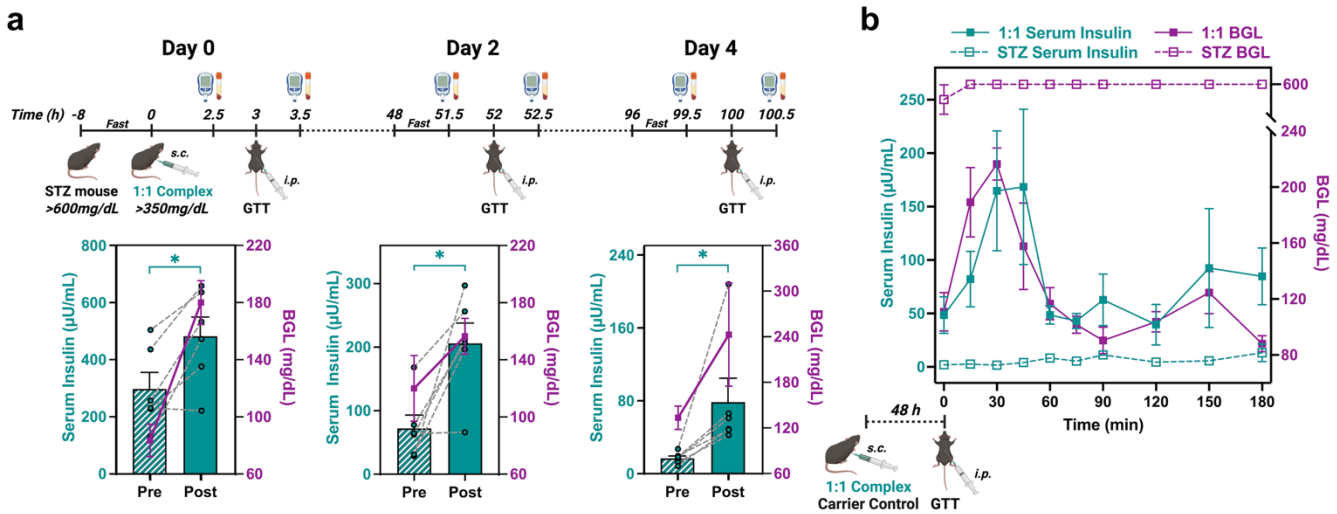

Figure 4: (a) Approach to measure changes in serum insulin resulting in STZ diabetic mice upon glucose challenge at D0, D2, and D4 following treatment with the Insulin-Dendrimer nanocomplex formulated at a charge ratio of 1:1. Serum insulin and blood glucose were measured 30 minutes prior to (*Pre*) and 30 minutes following (*Post*) administering IPGTT. Studies performed in 3 cohorts of mice for each treatment (n=6/cohort), with each cohort used for one of the timepoints (n=6/group, mean ± SEM shown, *- P<0.05 from a paired Student's t-test). **(b)** Kinetic profile of serum insulin levels and blood glucose in STZ diabetic mice for an IPGTT performed 48 hours after treatment with the Insulin-Dendrimer nanocomplex formulated at a charge ratio of 1:1 (*solid lines*) or a control of the Dendrimer-Diol carrier alone (STZ control, *dashed lines*). Study was performed in 5 cohorts of mice per group (n=5/cohort) with each cohort yielding two timepoints shown in the curve according to the table in the supporting information (n=5/group/timepoint, mean ± SEM shown).

treatment with the 1:1 complex in conjunction with IPGTT (***Fig 4a***). Serum was collected from mice along with blood glucose measurements at 30 min prior and then 30 min following IPGTT. The presence of serum insulin prior to IPGTT on all 4 days supports continuous basal insulin availability from the depot, aligning with expectations for some level of release even under low glucose conditions. However, at day 0, 2, and 4 following treatment, serum insulin levels were significantly elevated 30 min following IPGTT. The increase in serum insulin concentration at day 0 (+160%), 2 (+290%), and 4 (460%) amounted to a significant elevation over pre-challenge levels on all days. The general trend was strengthened by pre- and post-IPGTT serum insulin measurements having been taken from the same mouse. STZ mice administered the Dendrimer-Diol carrier alone were verified to have serum insulin levels at or below the limits of ELISA detection both before and after IPGTT (***Fig S25***). This result assures that ELISA-detected insulin was arising from the depot and not due to a glucose response emanating from residual pancreatic function that may result were STZ not effective at ablating the pancreatic β cells.

To further assess the kinetics of insulin availability from the depot, serum insulin levels were next measured serially in cohorts of mice administered the 1:1 nanocomplex during an IPGTT conducted 48 h after treatment (***Fig 4b***). Cohorts of mice all identically treated were necessary due to the blood volume collection requirements for accurate detection. At each timepoint, blood glucose was measured and serum samples were collected. The general trend in blood glucose following challenge matched that seen for groups of mice tracked over the same time, verifying the validity of the cohort approach. Excitingly, even at 48 h after treatment with the 1:1 complex serum insulin was elevated with kinetics that corresponded to the increase in blood glucose from IPGTT, and declined along with blood glucose correction. The difference between the average serum insulin concentration at the initial time (49 μU/mL) and at the peak (169 μU/mL) accounted for an increase of ~340%; blood glucose levels rose from 110 mg/dL to 216 mg/dL for an increase of ~195% in this same time. STZ-induced mice administered only a carrier showed no increase in serum insulin upon IPGTT. These data support insulin bioavailability originating from the depot that directly corresponds to changes in blood glucose level. Such kinetics have not yet been reported in the literature of glucose-responsive insulin technologies to date, though spikes in serum insulin following glucose challenge have been shown.[49]

Serial Dosing for Long-Term Blood Glucose Control. The function of Insulin–Dendrimer nanocomplexes was also explored in the context of repeat dosing over the course of 5 weeks, with complexes dosed every 5 d (***Fig 5a***). At two and four days after administration of each dose, blood glucose was measured following a brief 3 h fast, included to correct for time since last

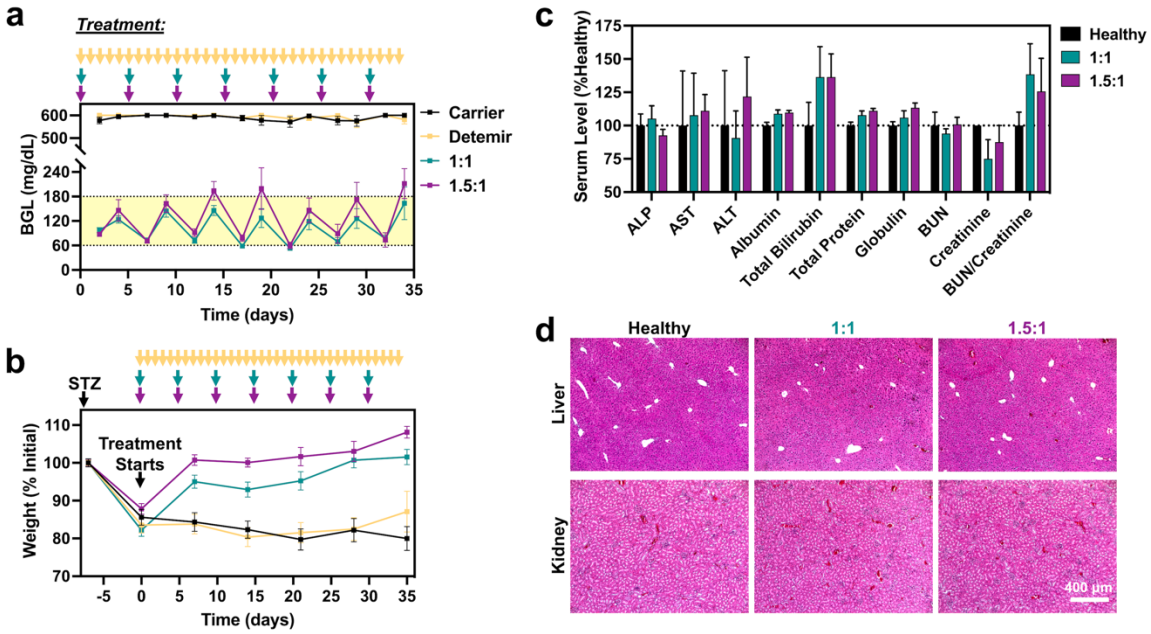

Figure 5: (a) Blood glucose levels in STZ diabetic mice upon serial dosing with the Insulin-Dendrimer nanocomplex formulations at a charge ratio of 1:1 or 1.5:1 administered every 5 days and compared to controls of mice treated every 5 days with the Dendrimer-Diol carrier or every day with a potency-matched dose of *Insulin Detemir*. Blood glucose levels were collected after a brief 3 h fast, with the yellow shaded region indicating the normal blood glucose range for a healthy mouse (n=10/group, mean ± SEM shown). **(b)** Animal weights were monitored throughout the study and presented relative to the pre-STZ weight of each mouse (n=10/group, mean ± SEM shown). **(c)** Serum chemistry to assess the toxicity of 1:1 and 1.5:1 nanocomplex formulations dosed serially for one month in healthy mice, with values of each marker presented relative to those for healthy mice (n=4/group, mean ± SEM shown, ANOVA performed with Tukey *post hoc* test for each analyte with no significance found). **(d)** Liver and kidney for 1:1 and 1.5:1 nanocomplex formulations dosed serially for one month in healthy mice.

meal and ensure gastric emptying. Using this dosing and assessment protocol, both 1:1 and 1.5:1 complexes maintained mice within a normoglycemic range (60-180 mg/dL for healthy mice) throughout the study, with a comparative improvement for the time-in-range upon treatment with the 1:1 formulation. The same previously established potency-matched daily dose of *Insulin Detemir*, determined based on its ability to elicit a similar blood glucose correction in overnight-fasted mice, did not provide sustained blood glucose correction. The mice treated with Insulin–Dendrimer nanocomplexes also had improved body condition, better grooming, reduced polyuria, and were of noticeably better health status than either the carrier control or *Insulin Detemir* groups. Indeed, mice treated with the Insulin–Dendrimer nanocomplexes recovered to their pre-STZ body weights following only a week of treatment whereas the carrier control and *Insulin Detemir* mice maintained body weights ~20% reduced from their pre-STZ levels (***Fig 5b***).

In order to further establish feasibility of serial redosing with the Insulin–Dendrimer nanocomplexes for long-term blood glucose control, these were dosed repeatedly in healthy mice for one month, after which serum chemistry was measured from samples collected at the study endpoint (***Fig 5c***). These studies were performed in healthy mice to avoid confounding influence from the toxic effects of STZ on health status. Serum markers of liver and kidney function were selected for profiling, showing no significant differences observed for any of the markers relative to healthy mice treated with saline. Likewise, endpoint histology of liver and kidney tissue following serial dosing for one month revealed normal tissue structures with no histological abnormalities (***Fig 5d***). These findings support limited impact from serial redosing of the Insulin–Dendrimer nanocomplexes on the metabolic function or overall health status in key organs associated with insulin signaling and clearance.[51,52] In particular, liver inflammation has been a key barrier in the development of other synthetically modified insulins,[53] and the lack of any inflammation here is therefore encouraging. It is envisioned that the Insulin–Dendrimer forms a nanoprecipitated depot following injection, similar to the mechanism of protraction for *Insulin Glargine*. A post-mortem search of the subcutaneous area following serial injection revealed no signs of inflammation or material accumulation, and thus the injection site (which varied slightly with every administration) was not able to be collected for analysis of local inflammation or material retention by histology.

PAMAM dendrimers are known to have hemolytic properties, as their highly cationic surface charge can

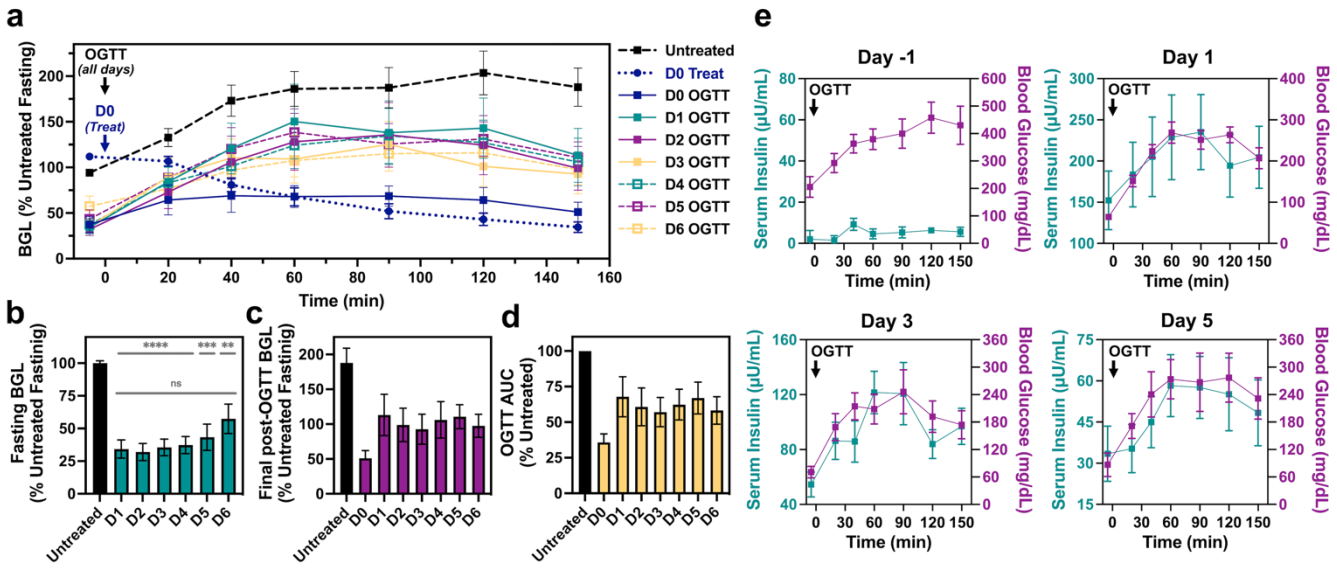

Figure 6: (a) Relative blood glucose levels in alloxan-treated diabetic swine (n=6) exposed to an oral glucose tolerance test (OGTT) administered at t=0, with all blood glucose levels normalized to fasted blood glucose levels for each individual untreated pig. The initial OGTT response for 2 days prior to treatment was measured for each individual pig, averaged, and plotted as the untreated control (*black dashed trace*). On D0, the Insulin-Dendrimer nanocomplex formulation at a charge ratio of 1:1 was first administered and blood glucose was first monitored for 3 h prior to OGTT (*blue dashed trace*). OGTT was then performed on D0 and each subsequent day (D1-D6) for a week following initial treatment with the Insulin-Dendrimer nanocomplex. **(b)** Fasting blood glucose level, **(c)** final blood glucose level at 150 minutes after OGTT, and **(d)** the AUC for each OGTT in the cohort of swine prior to treatment (*untreated*) and for OGTT performed in the days (D0-D6) following treatment with the Insulin-Dendrimer nanocomplex. **(e)** Kinetics of serum insulin and blood glucose levels for diabetic swine during the course of OGTT studies performed prior to the treatment (day -1) and on days 1, 3, and 5 following treatment with the Insulin-Dendrimer nanocomplex. (n=6 pigs, mean ± SEM shown for each data point in every panel).

interact with and disrupt red blood cell membranes.[54] This could present safety concerns in the context of translation of this current technology. A hemolysis assay was thus performed for Insulin-DiPBA and Dendrimer-Diol individually at concentrations ~1x-5x their maximum possible blood concentrations at the dosing levels used in mice (***Fig S26***). No hemolysis was observed for either component in these studies. For the Dendrimer-Diol, this result is attributed to the highly reduced surface charge due to modification of ~80% of the terminal PAMAM amino groups with the diol.

Blood Glucose Control in Ossabaw Minipigs. To assess the translational potential of the 1:1 Insulin–Dendrimer nanocomplex in a human-sized subject, a study was performed in alloxan-induced insulin-deficient 11-14 month-old Ossabaw minipigs with body weights of ~41-59 kg (~90-130 pounds, *n=6*). Alloxan is commonly used in pigs to recreate insulin-deficiency and hyperglycemia, pathological features of type 1 diabetes, due to its lower rate of mortality than STZ.[55] Following alloxan treatment and blood glucose stabilization, a baseline oral glucose tolerance test (OGTT) administered *via* gavage was performed for two consecutive days on each pig in an overnight-fasted state with no insulin treatment to determine the baseline untreated blood glucose response against which to compare each animal following treatment (***Fig 6a***). The average untreated fasting blood glucose levels for all swine at the study outset was 228 ± 43 mg/dL. Normal fasting blood glucose for healthy Ossabaw swine is in the range of roughly 57-71 mg/dL.[56] As such, alloxan treatment successfully induced hyperglycemia reminiscent of an insulin-deficient diabetic state. On the treatment day (D0), overnight-fasted swine were treated with the 1:1 Insulin–Dendrimer formulation at an insulin dose of ~0.8-0.9 mg/kg; the exact dose was determined specifically for each animal using reported methods for allometric scaling of insulin dose to account for the difference in size and body surface area of mice and swine.[57,58] Following treatment, blood glucose levels were reduced to ~35% of their initial fasted levels; after 3 h, the average blood glucose level for pigs was in the range of 71 ± 12 mg/dL, within the range expected for healthy swine.

Three hours following treatment with the Insulin–Dendrimer formulation, a D0 OGTT was performed (***Fig 6a***). Subsequent rounds of OGTT were performed on overnight-fasted swine for 6 additional days (D1-D6) to evaluate the effectiveness of a single dose of the formulation for one week of blood glucose control.

Blood glucose levels were generally reduced throughout the course of the week following treatment. This is most strongly evidenced by fasting blood glucose levels (***Fig 6b***) that were ~32% of untreated fasting levels (73 ± 15 mg/dL) in the early days following treatment. Though some elevation was seen over time, fasting blood glucose levels showed sustained control, even at D6 with levels that were ~57% of the untreated fasting blood glucose levels. The final blood glucose values for swine, collected at 150 min following OGTT, were also reduced to roughly half of their level in the untreated control state throughout D1-D6 following treatment (***Fig 6c***). The blood glucose levels from the OGTT performed at D0 were slightly depressed relative to subsequent days, likely due to increased insulin release following its initial administration. Dosing and injection volume could be further optimized in subsequent studies to limit the extent of initial burst release, though it is at the same time encouraging that swine did not exhibit signs of hypoglycemia resulting from administration of the Insulin–Dendrimer formulation. Overall, responsiveness as measured by the AUC throughout OGTT also was consistently reduced on D1-D6 following treatment compared to the untreated levels (***Fig 6d***).

Serum insulin levels were furthermore quantified during the course of OGTT on each day of the study (***Fig 6e***). Prior to treatment with the Insulin–Dendrimer formulation (D-1), serum insulin levels were near or below the limits of ELISA detection and did not show any corresponding increase in response to OGTT. These data confirm effective loss of insulin-secreting function in alloxan-treated swine. Following treatment with the Insulin–Dendrimer formulation, serum insulin levels were quantifiable, and more importantly were correlated with blood glucose levels during the course of OGTT (***Fig 6e***). As was observed in mouse studies, these data again point to glucose-triggered release of Insulin-DiPBA from the depot and increased serum insulin availability. Whereas the IPGTT in mouse studies indicated some lag in insulin levels following the increase in glucose, the serum insulin and blood glucose levels following OGTT in swine tracked more closely; this is likely due to the comparatively slower rate of glucose absorption for oral versus intraperitoneal administration.[59] It is noted that the serum insulin concentration released from the depot over the course of the OGTT decreased with time following treatment; these insulin levels were still effective in normalizing fasting blood glucose and controlling glucose levels throughout each OGTT cycle (***Fig S27***). Accordingly, in a human-sized animal model, the results support week-long blood glucose control and glucose-responsive function of this Insulin–Dendrimer nanocomplex formulation, both of which have never before been reported at this scale.

Conclusions

Ensuring accurate blood glucose control is central to diabetes management, with efforts to achieve such control also having a requirement that therapies are easily administered with a reasonable dosing schedule. The impactful results from weekly antidiabetogenic agents (e.g., GLP-1 analogues)[60] points to the utility of a once-weekly injectable to better manage diabetes. Similarly, the long-sought approach to achieve glucose-responsive insulin therapy would offer a more autonomous route to ensure accurate and temporarily relevant insulin dosing. Herein, the coupling of electrostatic and dynamic-covalent interactions between an insulin analogue bearing a high-affinity glucose-binding motif and a synthetic diol-modified dendrimer was shown to drive nanocomplex formation under physiological conditions, with this complexation susceptible to competition from glucose to release insulin. The resulting material constitutes an easily injected, low-viscosity formulation that forms a long-lasting depot capable of responding to repeated glucose challenges for up to a week following a single dose without significant hypoglycemia. The interplay of both electrostatic and dynamic-covalent interactions is key to the observed glucose-responsive and long-lasting function. Importantly, serum insulin levels in both diabetic mice and swine were correlated with increases in glucose level. The approach thus offers promise for multi-day glucose-responsive blood glucose control; serial dosing for one month showed no signs of toxicity. Accordingly, this technology simultaneously delivers on two long-sought goals for better blood glucose management in offering both glucose-responsive *and* multi-day blood glucose control from a single facile injection.

Though results from the current study are encouraging, there are several remaining challenges that must be addressed prior to clinical implementation of this general approach in the context of serial, and perhaps life-long, insulin therapy. Along with a reduction in insulin receptor binding affinity and signaling potency that is not ideal, the multi-step synthesis to prepare Insulin-DiPBA entails use of an expensive and bulky DBCO-modified intermediate and multiple rounds of purification to yield the final modified insulin. Future work will explore higher yielding one-step modification routes, including alternative bioconjugate, chemoenzymatic, or total synthesis approaches.[61–63] The extensive use of PAMAM and related cationic macromolecules in gene

therapy likewise points to a need to consider the possible toxicity of this component alongside its limited biodegradation and possible accumulation *in vivo*.[64] It has been shown that modifying the surface of PAMAM dendrimers improves compatibility;[65,66] the extensive diol modification of the Dendrimer-Diol may thus support compatibility of the current formulation. However, future research efforts should seek carriers that are more readily degraded and/or cleared to limit the risk of chronic accumulation from repeated administration, an especially important consideration given the serial and life-long nature of insulin therapy.

Experimental Methods

Detailed experimental methods can be found in the online supporting information.

Acknowledgments

MJW gratefully acknowledges funding support for this work from the Juvenile Diabetes Research Foundation (5-CDA-2020-947-A-N), the Helmsley Charitable Trust (grants 2019PG-T1D016 and 2102-04994), the American Diabetes Association Pathway Accelerator Award (1-19-ACE-31), and a National Science Foundation CAREER award (BMAT, 1944875). JJ and KM were supported by the National Institute for Research of Metabolic and Cardiovascular Diseases of the Czech Republic (Program EXCELES, Project LX22NPO5104, funded by the European Union-Next Generation EU) and by the Czech Academy of Sciences (Research Project RVO:6138963). Schematics in Fig 1 and Fig 4 created using BioRender.com.

Author contributions

SX and YX contributed equally to this work. SX, YX, and MJW conceived of ideas and designed the studies. SX, YX, DL, BF, MAA, KM, RCO, JJ, MS, MA, and MJW designed/conducted experiments and contributed to data collection and analysis. SX, YX, and MJW wrote the manuscript. All authors reviewed the manuscript and approved of its submission.

Competing interests

SX, YX, and MJW. are co-inventors on provisional patent filings related to this technology. All other authors declare no competing interests.

Other Information

Supplementary information The online version contains supplementary material available at:

Correspondence and requests for materials should be addressed to Matthew J. Webber, mwebber@nd.edu

References

[1] M. A. B. Khan, M. J. Hashim, J. K. King, R. D. Govender, H. Mustafa, J. Al Kaabi, *J. Epidemiol. Glob. Health* **2020**, *10*, 107.
[2] X. Lin, Y. Xu, X. Pan, J. Xu, Y. Ding, X. Sun, X. Song, Y. Ren, P.-F. Shan, *Sci. Rep.* **2020**, *10*, 14790.
[3] J. L. Harding, M. E. Pavkov, D. J. Magliano, J. E. Shaw, E. W. Gregg, *Diabetologia* **2019**, *62*, 3.
[4] R. A. DeFronzo, E. Jacot, E. Jequier, E. Maeder, J. Wahren, J. P. Felber, *Diabetes* **1981**, *30*, 1000.
[5] A. Janež, C. Guja, A. Mitrakou, N. Lalic, T. Tankova, L. Czupryniak, A. G. Tabák, M. Prazny, E. Martinka, L. Smircic-Duvnjak, *Diabetes Ther.* **2020**, *11*, 387.
[6] M. Peyrot, A. H. Barnett, L. F. Meneghini, P.-M. Schumm-Draeger, *Diabet. Med.* **2012**, *29*, 682.
[7] R. G. McCoy, H. K. Van Houten, J. Y. Ziegenfuss, N. D. Shah, R. A. Wermers, S. A. Smith, *Diabetes Care* **2012**, *35*, 1897.
[8] M. Muggeo, G. Zoppini, E. Bonora, E. Brun, R. C. Bonadonna, P. Moghetti, G. Verlato, *Diabetes Care* **2000**, *23*, 45.
[9] D. R. Owens, *Nat. Rev. Drug Discov.* **2002**, *1*, 529.
[10] P. Kurtzhals, E. Nishimura, H. Haahr, T. Høeg-Jensen, E. Johansson, P. Madsen, J. Sturis, T. Kjeldsen, *Trends Pharmacol. Sci.* **2021**, *42*, 620.
[11] J. Kesavadev, B. Saboo, M. B. Krishna, G. Krishnan, *Diabetes Ther.* **2020**, *11*, 1251.
[12] O. Didyuk, N. Econom, A. Guardia, K. Livingston, U. Klueh, *J. Diabetes Sci. Technol.* **2021**, *15*, 676.
[13] Q. Wu, L. Wang, H. Yu, J. Wang, Z. Chen, *Chem. Rev.* **2011**, *111*, 7855.
[14] M. A. VandenBerg, M. J. Webber, *Adv. Healthc. Mater.* **2019**, *8*, e1801466.
[15] J. Wang, Z. Wang, J. Yu, A. R. Kahkoska, J. B. Buse, Z. Gu, *Adv. Mater.* **2020**, *32*, e1902004.
[16] M. J. Webber, D. G. Anderson, *J. Drug Target.* **2015**, *23*, 651.
[17] Y. Xiang, B. Su, D. Liu, M. J. Webber, *Adv. Ther.* **2023**, DOI 10.1002/adtp.202300127.
[18] R. Ma, L. Shi, *Polym. Chem.* **2014**, *5*, 1503.
[19] W. L. A. Brooks, B. S. Sumerlin, *Chem. Rev.* **2016**, *116*, 1375.
[20] B. Marco-Dufort, M. W. Tibbitt, *Materials Today Chemistry* **2019**, *12*, 16.
[21] W. L. A. Brooks, C. C. Deng, B. S. Sumerlin, *ACS Omega* **2018**, *3*, 17863.
[22] Y. Xiang, S. Xian, R. C. Ollier, S. Yu, B. Su, I. Pramudya, M. J. Webber, *J. Control. Release* **2022**, *348*, 601.
[23] R. Esfand, D. A. Tomalia, *Drug Discov. Today* **2001**, *6*, 427.
[24] F. Abedi-Gaballu, G. Dehghan, M. Ghaffari, R. Yekta, S. Abbaspour-Ravasjani, B. Baradaran, J. E. N. Dolatabadi, M. R. Hamblin, *Appl Mater Today* **2018**, *12*, 177.
[25] H. Kheraldine, O. Rachid, A. M. Habib, A.-E. Al Moustafa, I. F. Benter, S. Akhtar, *Adv. Drug Deliv. Rev.* **2021**, *178*, 113908.
[26] J. Pettus, T. Santos Cavaiola, W. V. Tamborlane, S. Edelman, *Diabetes. Metab. Res. Rev.* **2016**, *32*, 478.
[27] T. Heise, C. Mathieu, *Diabetes Obes. Metab.* **2017**, *19*, 3.
[28] A. Y. Y. Cheng, D. K. Patel, T. S. Reid, K. Wyne, *Adv. Ther.* **2019**, *36*, 1018.
[29] A. W. Krug, S. A. G. Visser, K. Tsai, B. Kandala, C. Fancourt, B. Thornton, L. Morrow, N. C. Kaarsholm, H. S. Bernstein, S. A. Stoch, M. Crutchlow, D. E. Kelley, M. Iwamoto, *Clin. Pharmacol. Ther.* **2019**, *105*, 417.
[30] D. H.-C. Chou, M. J. Webber, B. C. Tang, A. B. Lin, L. S.

Thapa, D. Deng, J. V. Truong, A. B. Cortinas, R. Langer, D. G. Anderson, *Proc. Natl. Acad. Sci. U. S. A.* **2015**, *112*, 2401.
[31] P. Home, P. Kurtzhals, *Expert Opin. Pharmacother.* **2006**, *7*, 325.
[32] H. G. Kuivila, J. F. Reuwer Jr, J. A. Mangravite, *Can. J. Chem.* **1963**, *41*, 3081.
[33] C. Y. Wong, H. Al-Salami, C. R. Dass, *J. Pharm. Pharmacol.* **2020**, *72*, 1667.
[34] Y. Shen, A. Joachimiak, M. R. Rosner, W.-J. Tang, *Nature* **2006**, *443*, 870.
[35] M. Takayama, K. Yamauchi, T. Aizawa, *Diabet. Med.* **2014**, *31*, 375.
[36] M. Akbarian, Y. Ghasemi, V. N. Uversky, R. Yousefi, *Int. J. Pharm.* **2018**, *547*, 450.
[37] L. Sciacca, M. F. Cassarino, M. Genua, G. Pandini, R. Le Moli, S. Squatrito, R. Vigneri, *Diabetologia* **2010**, *53*, 1743.
[38] S. C. Ong, A. Belgi, A. L. Merriman, C. A. Delaine, B. van Lierop, S. Andrikopoulos, A. J. Robinson, B. E. Forbes, *Front. Endocrinol.* **2022**, *13*, 907864.
[39] B. Draznin, *Diabetologia* **2010**, *53*, 229.
[40] V. Yesilyurt, M. J. Webber, E. A. Appel, C. Godwin, R. Langer, D. G. Anderson, *Adv. Mater.* **2016**, *28*, 86.
[41] F. Zhang, J. Trent Magruder, Y.-A. Lin, T. C. Crawford, J. C. Grimm, C. M. Sciortino, M. A. Wilson, M. E. Blue, S. Kannan, M. V. Johnston, W. A. Baumgartner, R. M. Kannan, *J. Control. Release* **2017**, *249*, 173.
[42] S. Hvidt, *Biophys. Chem.* **1991**, *39*, 205.
[43] S. M. Patil, D. A. Keire, K. Chen, *AAPS J.* **2017**, *19*, 1760.
[44] R. Coppolino, S. Coppolino, V. Villari, *J. Pharm. Sci.* **2006**, *95*, 1029.
[45] B. L. Furman, *Curr. Protoc. Pharmacol.* **2015**, *70*, 5.47.1.
[46] L. J. Hirsch, K. W. Strauss, *Clin. Diabetes* **2019**, *37*, 227.
[47] E. Cengiz, W. V. Tamborlane, *Diabetes Technol. Ther.* **2009**, *11 Suppl 1*, S11.
[48] S. Xian, M. A. VandenBerg, Y. Xiang, S. Yu, M. J. Webber, *ACS Biomater Sci Eng* **2022**, *8*, 4873.
[49] L. R. Volpatti, A. L. Facklam, A. B. Cortinas, Y.-C. Lu, M. A. Matranga, C. MacIsaac, M. C. Hill, R. Langer, D. G. Anderson, *Biomaterials* **2021**, *267*, 120458.
[50] J. L. Knopp, L. Holder-Pearson, J. G. Chase, *J. Diabetes Sci. Technol.* **2019**, *13*, 597.
[51] P. M. Titchenell, Q. Chu, B. R. Monks, M. J. Birnbaum, *Nat. Commun.* **2015**, *6*, 7078.
[52] R. Rabkin, M. P. Ryan, W. C. Duckworth, *Diabetologia* **1984**, *27*, 351.
[53] A. Muñoz-Garach, M. Molina-Vega, F. J. Tinahones, *Diabetes Ther.* **2017**, *8*, 9.
[54] D. Luong, P. Kesharwani, R. Deshmukh, M. C. I. Mohd Amin, U. Gupta, K. Greish, A. K. Iyer, *Acta Biomater.* **2016**, *43*, 14.
[55] M. Radenković, M. Stojanović, M. Prostran, *J. Pharmacol. Toxicol. Methods* **2016**, *78*, 13.
[56] R. Mazor, A. Babkin, P. J. Littrup, M. Alloush, M. Sturek, J. P. Byrd, E. Hernandez, H. Bays, E. Grunvald, S. G. Mattar, *Surg. Obes. Relat. Dis.* **2023**, *19*, 374.
[57] A. B. Nair, S. Jacob, *J. Basic Clin. Physiol. Pharmacol.* **2016**, *7*, 27.
[58] V. Sharma, J. H. McNeill, *Br. J. Pharmacol.* **2009**, *157*, 907.
[59] L. Small, A. Ehrlich, J. Iversen, S. P. Ashcroft, K. Trošt, T. Moritz, B. Hartmann, J. J. Holst, J. T. Treebak, J. R. Zierath, R. Barrès, *Mol Metab* **2022**, *57*, 101440.
[60] J. P. H. Wilding, R. L. Batterham, S. Calanna, M. Davies, L. F. Van Gaal, I. Lingvay, B. M. McGowan, J. Rosenstock, M. T. D. Tran, T. A. Wadden, S. Wharton, K. Yokote, N. Zeuthen, R. F. Kushner, STEP 1 Study Group, *N. Engl. J. Med.* **2021**, *384*, 989.
[61] M. Østergaard, N. K. Mishra, K. J. Jensen, *Chemistry* **2020**, *26*, 8341.
[62] A. Fryszkowska, C. An, O. Alvizo, G. Banerjee, K. A. Canada, Y. Cao, D. DeMong, P. N. Devine, D. Duan, D. M. Elgart, I. Farasat, D. R. Gauthier, E. N. Guidry, X. Jia, J. Kong, N. Kruse, K. W. Lexa, A. A. Makarov, B. F. Mann, E. M. Milczek, V. Mitchell, J. Nazor, C. Neri, R. K. Orr, P. Orth, E. M. Phillips, J. N. Riggins, W. A. Schafer, S. M. Silverman, C. A. Strulson, N. Subramanian, R. Voladri, H. Yang, J. Yang, X. Yi, X. Zhang, W. Zhong, *Science* **2022**, *376*, 1321.
[63] J. A. Karas, J. D. Wade, M. A. Hossain, *Chem. Rev.* **2021**, *121*, 4531.
[64] A. Janaszewska, J. Lazniewska, P. Trzepiński, M. Marcinkowska, B. Klajnert-Maculewicz, *Biomolecules* **2019**, *9*, DOI 10.3390/biom9080330.
[65] R. Jevprasesphant, J. Penny, R. Jalal, D. Attwood, N. B. McKeown, A. D'Emanuele, *Int. J. Pharm.* **2003**, *252*, 263.
[66] M. Ciolkowski, J. F. Petersen, M. Ficker, A. Janaszewska, J. B. Christensen, B. Klajnert, M. Bryszewska, *Nanomedicine* **2012**, *8*, 815.